RESEARCH PAPER

# Beyond the limbic system: disruption and functional compensation of large-scale brain networks in patients with anti-LGI1 encephalitis

Josephine Heine,[1] Harald Prüss,[1,2] Ute A Kopp,[1] Florian Wegner,[3] Florian Then Bergh,[4] Thomas Münte,[5] Klaus-Peter Wandinger,[5,6] Friedemann Paul,[1,7,8] Thorsten Bartsch,[9] Carsten Finke[1,8,10]

## ABSTRACT

**Objective** Hippocampal inflammation in anti-LGI1 encephalitis causes memory deficits, seizures and behavioural abnormalities. Recent findings suggest that extralimbic brain areas are additionally affected and that patients also suffer from non-limbic cognitive symptoms. Moreover, up to 60% of patients show no structural MRI abnormalities in the acute disease stage. We therefore investigated whether functional connectivity analyses can identify brain network changes underlying disease-related symptoms.

**Methods** We studied 27 patients and a matched healthy control group using structural and functional MRI. Intrinsic functional networks were analysed using Independent Component Analysis and Dual Regression. Cognitive testing covered working memory, episodic memory, attention and executive function.

**Results** Our analysis revealed functional connectivity alterations in several large-scale networks, including the default mode network (DMN) which showed an aberrant structure-function relationship with the damaged hippocampus. In addition, connectivity in the sensorimotor, salience and higher visual networks was impaired independent of hippocampal damage. Increased connectivity in ventral and dorsal DMN regions significantly correlated with better memory performance. In contrast, stronger connectivity of the insula with the salience network and DMN was linked to impaired memory function.

**Conclusions** Anti-LGI1 encephalitis is associated with a characteristic pattern of widespread functional network alterations. Increased DMN connectivity seems to represent a compensatory mechanism for memory impairment induced by hippocampal damage. Network analyses may provide a key to the understanding of clinical symptoms in autoimmune encephalitis and reveal changes of brain function beyond apparent structural damage.

Check for updates

## INTRODUCTION

Limbic encephalitis with neuronal autoantibodies targeting the leucine-rich glioma-inactivated 1 (LGI1) protein affects one of the brain's major hubs for higher-order cognition: the hippocampus. Patients consequently suffer from pronounced memory deficits, seizures and neuropsychiatric abnormalities.[1–3] While the term *limbic encephalitis* suggests a pathology limited to limbic brain structures such as the hippocampus and amygdala, recent clinical and imaging findings indicate an involvement of a wider network of brain areas.[4–7]

In anti-LGI1 encephalitis, faciobrachial dystonic seizures (FBDS) frequently precede the onset of limbic encephalitis.[8–10] Imaging analyses during this early disease stage revealed alterations of basal ganglia metabolism using FDG-PET[6 11] and transient T1 and T2 basal ganglia hyperintensities contralateral to the side of FBDS.[6] Another recent study linked hypermetabolism of the primary motor cortex and frontal cortex EEG changes to contralateral FBDS.[5]

During the limbic encephalitis stage of the disease, hippocampal T2/FLAIR hyperintense signal alterations are observed in most patients and frequently evolve into permanent hippocampal atrophy with persistent cognitive dysfunction.[4 9 12 13] These imaging findings correspond to the predominant expression of LGI1 in the hippocampus[2 14] and underpin hippocampal vulnerability in anti-LGI1 encephalitis. However, previous studies reported a range of 20%–60% of patients without structural MRI abnormalities in this disease stage despite an impaired memory function,[4 5 11 15] and whole brain analyses of grey and white matter integrity revealed no extrahippocampal damage in patients with anti-LGI1 encephalitis.[4] In contrast, recent FDG-PET studies provide first evidence for altered metabolism in the prefrontal cortex, anterior cingulate, parietal cortex and cerebellum.[5 16] In addition, the majority of patients present with extralimbic (non-memory) cognitive impairments, such as deficits of attention and executive dysfunction. Together, these findings illustrate the currently insufficient understanding of the relationship between affected brain regions and clinical symptoms in anti-LGI1 encephalitis.

Given these findings, we hypothesised that patients with anti-LGI1 encephalitis suffer from disruptions of large-scale functional networks, induced either by hippocampal damage or by more widespread antibody-mediated LGI1 dysfunction, thereby contributing to extralimbic clinical manifestations. We therefore used resting state functional MRI and Independent Component Analysis (ICA) to study the relationship of intrinsic connectivity alterations and cognitive

BMJ

1

**Table 1** Patient characteristics

| | | |
|---|---|---|
| Age (mean±SD) | 65.8±11.4 years | |
| Sex | 18 male, 9 female | |
| mRS score (median (range)) | 2 (0–4) | |
| Follow-up time (mean±SD) | 25.9±16.7 months | |
| EEG abnormalities | 20/27 (74%) | |
| **Symptoms in acute phase** | | |
| Cognitive | | |
| Memory impairment | 27/27 (100%) | |
| Disorientation, confusion | 20/27 (74%) | |
| Affective symptoms | 7/27 (26%) | |
| Behavioural abnormalities | 7/27 (26%) | |
| Sleep disturbance | 6/27 (22%) | |
| Seizures | 26/27 (96%) | |
| FBDS | 13/26 (50%) | |
| Pilomotor/autonomic | 6/26 (23%) | |
| Complex focal | 6/26 (23%) | |
| Generalised tonic-clonic | 5/26 (19%) | |
| **MRI abnormalities** | **Acute phase** | **Follow-up*** |
| Mild global atrophy | 1/27 (4%) | 6/27 (22%) |
| Periventricular white matter lesions | 1/27 (4%) | 1/27 (4%) |
| Basal ganglia hyperintensities | 0 | 0 |
| Hippocampal hyperintensities (T2/FLAIR) | | |
| Unilateral | 8/27 (30%) | 5/27 (19%) |
| Bilateral | 13/27 (48%) | 9/27 (33%) |
| Conversion to hippocampal atrophy | | |
| Unilateral | – | 9/27 (33 %) |
| Bilateral | – | 15/27 (56 %) |

*Time of study MRI.
FBDS, faciobrachial dystonic seizures; mRS, modified Rankin Scale.

symptoms. This data-driven analysis allows the identification of functional networks, that is, consistently detectable ensembles of distributed brain regions whose spontaneous activation patterns exhibit a high degree of temporal correlation.[17] These functional networks link to higher-order information processing to predict and respond to environmental demands.[18] For this reason, they are of major interest in the study of neurological and psychiatric diseases, including autoimmune encephalitis.[19] Corresponding to the clinical picture, we were primarily interested in resting-state networks (RSN) implicated in cognition and motor functions, that is, the default mode network (DMN), the salience network (SN), the frontoparietal (FPN) and the sensorimotor network.

## METHODS
### Participants
Twenty-seven patients with anti-LGI1 encephalitis (9 women/18 men; mean age 65.8 years (SD 11.4, range 38–80); mean of 14.8 years of formal education (SD 2.4)) were studied at Charité University Hospital Berlin (n=16) and the University Hospital Schleswig-Holstein in Kiel (n=11). Data of 26/27 patients have been reported previously.[4] Diagnosis was established based on the proposed criteria of characteristic clinical presentation, cerebrospinal fluid findings, neuroimaging changes and autoantibody detection.[20] Disease symptoms during the acute stage and clinical MRI findings are summarised in table 1. The modified Rankin Scale (mRS) was used to assess symptom severity. Follow-up time was defined as the time span between the onset of first symptoms and

the study MRI. Clinical and neuropsychological data as well as structural MRI analyses of these patients have previously been reported.[4] At the time of study MRI, patients received immunosuppressive drugs (n=5), anticonvulsive medication (n=5) or both (n=7; see online supplementary table 1). All patients were seizure-free. The control group consisted of 27 healthy individuals without history of neurological and psychiatric disease was similar to patients with regard to age (mean 64.3 years (SD 12.0); p=0.66), sex and education (mean 13.4 years (SD 12.0); p=0.07). Healthy controls were matched at each study site, providing the same ratio of patients to healthy controls at each location. All participants provided informed written consent.

### Neuropsychological assessment
Cognitive testing comprised (1) verbal short-term memory (digit span test; Wechsler Memory Scale—Revised), (2) verbal and non-verbal episodic memory (Rey Auditory Verbal Learning Test (RAVLT), Rey-Osterrieth Complex Figure Test (ROCF) & Boston Scoring System), (3) a test of tonic and phasic alertness as well as (4) executive functions (semantic fluency, Stroop test, computerised Go/No-Go test of the TAP battery).

### Image acquisition
MRI was performed at the Berlin Center for Advanced Neuro-imaging (BCAN) at Charité University Hospital Berlin using a 3T Tim Trio scanner (Siemens, Erlangen, Germany) equipped with a 12-channel phased array head coil. At the University Hospital in Kiel, MR images were acquired on a 3T Achieva scanner (Philips, Amsterdam, the Netherlands) with a 32-channel head coil. The neuroimaging protocol included structural and functional scans. We acquired a resting-state functional MRI scan using an echoplanar imaging sequence (EPI; TR=2250/3000 ms, TE=30 ms, 260/200 volumes, matrix size=64×64/80×80, 37/40 axial slices aligned to the bicommissural plane, slice thickness=3.4/3.5 mm, voxel size=3.4×3.4×3.4/3×3×3.5 mm³). For this resting-state sequence, participants were asked to lie still and keep their eyes closed. The acquisition time was ~10 min. The high-resolution T1-weighted structural scan (1×1×1 mm³) was collected using a magnetization-prepared rapid gradient echo sequence (MPRAGE; matrix size=240×240, 176 slices). Diffusion tensor imaging (DTI) data were acquired using a single-shot EPI sequence (voxel size 2×2×2 mm³, 61 slices, 64 diffusion directions, $b$ value=1000 s/mm²).

### Functional connectivity analysis
fMRI analysis was performed using the ICA and Dual Regression approach as implemented in the fMRIB Software Library (FSL 5.0 https://fsl.fmrib.ox.ac.uk/fsl/fslwiki). ICA is a data-driven method that decomposes a multivariate fMRI signal into single components with maximally independent spatial and temporal patterns. Resting state scans from the two study sites were preprocessed independently to account for differences in image acquisition. All scans were brain extracted, slice time corrected and underwent high-pass temporal filtering with a cut-off of 100 s. To correct for motion artefacts and ensure consistent mapping between voxels of individual scans, we performed FSL MCFLIRT motion correction. Both absolute (patients, 0.39±0.19 mm vs controls, 0.43±0.29 mm, p=0.61) and relative head motion (0.14±0.06 mm vs 0.16±0.08 mm, p=0.27) were not significantly different between groups. Next, all images were smoothed by a Gaussian Kernel of 6 mm full-width at half-maximum. After preprocessing, the

functional scan was first aligned to the individual's high resolution T1-weighted image (linear boundary-based registration), which was subsequently registered to the MNI152 standard space using nonlinear registration with 12 DOF and 10 mm warp resolution. FSL MELODIC V.3.14[21] was used to identify RSNs from the control group data. The estimation of the ICs was restricted to control group fMRI data to create a group ICA template unbiased towards disease-related changes. Voxel-wise between group comparisons were performed using dual regression.[22] During this step, a grey matter mask derived from all subjects using FSL FAST[23] restricted the analysis to cortical areas. To account for possible influences of the different MR scanners, 'acquisition site' was added as a covariate to the general linear model (GLM) for permutation testing using the FSL tool randomise.[24] Correlational analyses were likewise modelled in the GLM and tested for associations with disease severity (mRS), disease duration and cognitive scores. All statistical parametric maps were corrected for multiple comparisons using threshold-free cluster enhancement.[25] The threshold was set to $p < 0.05$. Images were created using MRIcron (http://people.cas.sc.edu/rorden/mricron/index.html) and Caret software (http://www.nitrc.org/projects/caret/). We additionally assessed hippocampal, whole brain and total grey matter volume and analysed white matter tracts using DTI and grey matter morphology using voxel-based morphometry (VBM) as described previously[4] to account for structural changes underlying functional alterations. Last, we performed an interaction analysis of hippocampal volume and functional connectivity to investigate differences in structure-function relationships between patients and controls.

### Statistical analyses

Statistical analyses were carried out using SPSS V.22.0 (SPSS). Cognitive results are reported with mean and standard error (SE). Between-group differences were analysed using independent samples t-tests.

## RESULTS

### Neuropsychological assessment

In comparison to healthy controls, patients were cognitively impaired in several neuropsychological domains (table 2). Patients had a significantly impaired working memory when compared with healthy controls (digit span test) and a substantial impairment in both verbal and visual learning and episodic memory (RAVLT/ROCF). Executive dysfunction became evident as increased error rate on the Go/No-Go test and a decreased semantic fluency. In contrast, the patients' response times were normal on the Go/No-Go test and not different from those of healthy controls on tests of tonic and phasic alertness.

### Structural MRI analyses

During the acute phase, hippocampal T2/FLAIR hyperintensities on routine MRI were seen in the majority of patients (21/27 patients (77.7%); unilateral in 8/27 patients (29.6%); bilateral in 13/27 patients (48.1%)), while in 6 patients (22.3%) no hippocampal abnormalities were present (table 1).

At the time of resting-state data acquisition (follow-up), initial hyperintensities evolved into unilateral (in 33.3%) or bilateral (55.6%) visually detectable hippocampal atrophy, while 11.1% of the patients showed no hippocampal atrophy. Volume measures revealed a significantly reduced right hippocampal volume (table 2). Furthermore, patients and controls did not differ on global measures of whole brain volume ($1.223 \times 10^6 \pm 0.33 \times 10^6$ mm³ vs $1.191 \times 10^6 \pm 0.29 \times 10^6$ mm³, p=0.697) and total grey matter volume ($0.567 \times 10^6 \pm 0.01 \times 10^6$ mm³ vs $0.591 \times 10^6 \pm 0.01 \times 10^6$ mm³, p=0.172) at follow-up. VBM analysis revealed no further cortical volume change and

**Table 2** Cognitive results and hippocampal volumes

| | Patients | Controls | t | P value |
|---|---|---|---|---|
| **Memory** | | | | |
| Working memory | | | | |
|   Digit span | 12.63 (±0.93) | 15.54 (±0.69) | t(51)=−2.51 | 0.015* |
| Verbal episodic memory (RAVLT) | | | | |
|   Supraspan | 5.38 (±0.42) | 7.48 (±0.41) | t(51)=−3.57 | 0.001** |
|   Sum score | 39.46 (±3.01) | 54.59 (±1.67) | t(51)=−4.44 | <0.001** |
|   Interference | 4.67 (±0.63) | 5.88 (±0.36) | t(51)=−1.69 | (0.102) |
|   Delayed recall | 6.27 (±1.04) | 11.78 (±0.56) | t(51)=−4.72 | <0.001** |
| Visual episodic memory (ROCF) | | | | |
|   Delayed recall | 15.63 (±1.91) | 25.86 (±1.24) | t(43)=−4.35 | <0.001** |
| **Attention** | | | | |
|   Tonic alertness (median, ms) | 309.24 (±16.35) | 281.58 (±11.09) | t(43)=1.43 | (0.16) |
|   Phasic alertness (median, ms) | 308.23 (±19.49) | 269.12 (±45.49) | t(45)=1.89 | (0.065) |
| **Executive function** | | | | |
|   Go/No-Go (median, ms) | 608.20 (±24.88) | 583.38 (±63.65) | t(37)=0.97 | (0.338) |
|   Go/No-Go (errors) | 3.00 (±1.09) | 0.35 (±0.11) | t(37)=2.77 | 0.008** |
|   Semantic fluency | 21.35 (±6.15) | 26.52 (±6.72) | t(46)=−2.78 | 0.008** |
| **Hippocampal volume** | | | | |
|   Left | 3566 (±127) mm³ | 3858 (±130) mm³ | t(52)=1.60 | (0.115) |
|   Right | 3448 (±152) mm³ | 4015 (±122) mm³ | t(52)=2.91 | 0.005** |

*P<0.05.
**P<0.01.
RAVLT, Rey Auditory Verbal Learning Test; ROCF, Rey Osterrieth Complex Figure Test; mean (±SE).
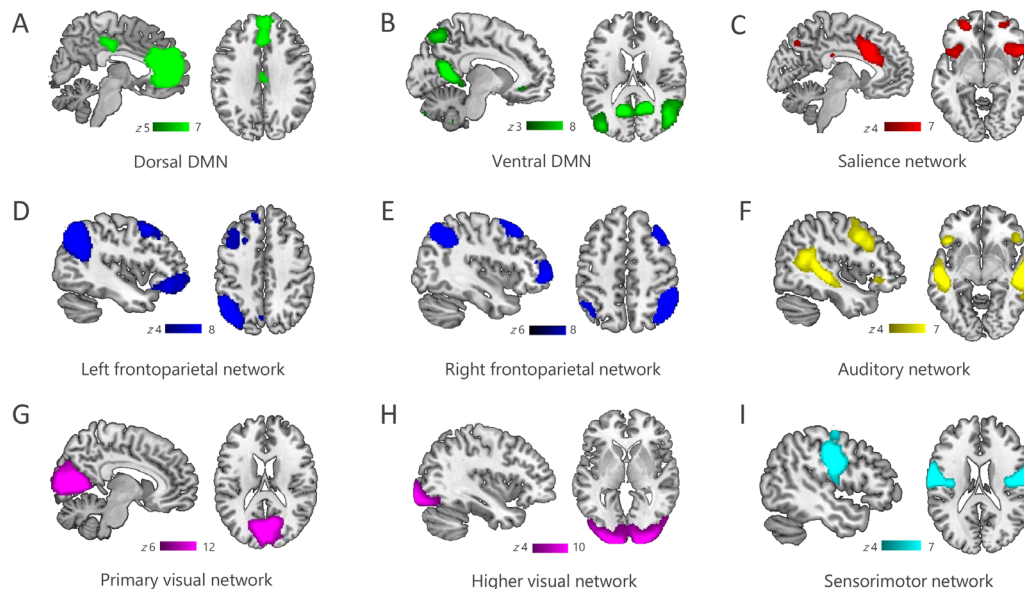
**Figure 1** Functional networks. Resting-state networks identified using Independent Component Analysis included the dorsal and ventral fractions of the DMN (A,B), the salience network (C), the lateralised frontoparietal networks (D,E), auditory and visual networks (F,G,H) as well as a sensorimotor network (I). DMN, default mode network.

there was no evidence of structural white matter damage as assessed using DTI.

### Functional connectivity MRI analyses

Following the investigation of structural integrity, we identified nine canonical RSNs, including the DMN, FPN, SN, sensorimotor network, auditory network as well as the primary and higher visual networks (figure 1A–I).[26 27] Aberrant functional connectivity was observed across several networks. We observed significantly increased functional connectivity in patients relative to controls in the dorsal and ventral DMN, the higher visual network and the sensorimotor network, while connectivity in the SN was reduced in patients (figure 2). Furthermore, connectivity within the dorsal and ventral DMN and the SN correlated with patients' memory performance (figure 3). No correlations were observed with follow-up time in any of the examined networks (median 25.9 months, range 1.0–118.2). These results are presented in more detail in the following paragraphs.

### Dorsal DMN

Within the dorsal DMN, cingulate and medial prefrontal cortex (mPFC) connectivity was bilaterally increased in patients (p=0.01; figure 2A). Higher connectivity was additionally observed between the dorsal DMN and more remote areas in the left precuneus and frontal cortex. Regarding memory function, higher DMN connectivity with left temporal areas and the cingulate cortex correlated with better working memory performance (digit span test, r=0.66, p=0.012; figure 3A).

### Ventral DMN

Patients had significantly higher precuneus connectivity within the ventral DMN (p<0.001; figure 2B). Moreover, patients showed increased connectivity of the ventral DMN with distributed frontal areas, including the insula, but also inferior temporal and right lateral occipital regions. These connectivity changes were associated with higher disease severity (mRS, $r_s$=0.81, p=0.031). Correlation analyses additionally revealed a negative association between insular involvement and

verbal memory performance: The higher the insular connectivity with this network, the fewer words were recalled on the verbal learning test (RAVLT supraspan, r=−0.46, p=0.026). In contrast, a coactivation of left temporal areas was—as previously observed in the dorsal DMN—positively correlated with verbal memory performance (RAVLT interference, r=0.92, p=0.005, figure 3B).

### Salience network

We observed decreased functional connectivity between the SN and left parietal areas in patients (p=0.029; figure 2C). A negative association was observed between cognitive performance and insular connectivity, that is, one of the major SN hubs. Specifically, higher connectivity of the left insula within the network related to worse working memory performance (digit span test, r=−0.72, p=0.032) and higher connectivity of the insula bilaterally was associated with poorer verbal learning performance (RAVLT sum score, r=−0.90, p=0.007) and poorer verbal episodic memory (RAVLT delayed recall, r=−0.88, p=0.002; figure 3B). A poor outcome in the memory domain was also related to the involvement of external DMN areas. Working memory performance was worse for higher connectivity between the SN and parietal default mode areas (digit span test, r=−0.72, p=0.032; figure 3A). In the same way, poor episodic memory performance was associated with increased SN connectivity with the temporal cortex, parietal cortex and subcortical structures, including the hippocampus (RAVLT sum score, r=−0.88, p=0.007, delayed recall, p=0.002; figure 3B). Unlike in the DMNs, a coactivation of lateral temporal areas correlated with higher disease severity (mRS, $r_s$=0.73, p=0.031).

### Sensorimotor and visual networks

Additionally, patients showed a higher connectivity of the *sensorimotor network* with left cerebellum (p=0.01) and of the *visual network* with right lateral occipital cortex (p=0.01). We observed no association of the sensorimotor network changes with the duration or frequency of FBDS events. No alterations
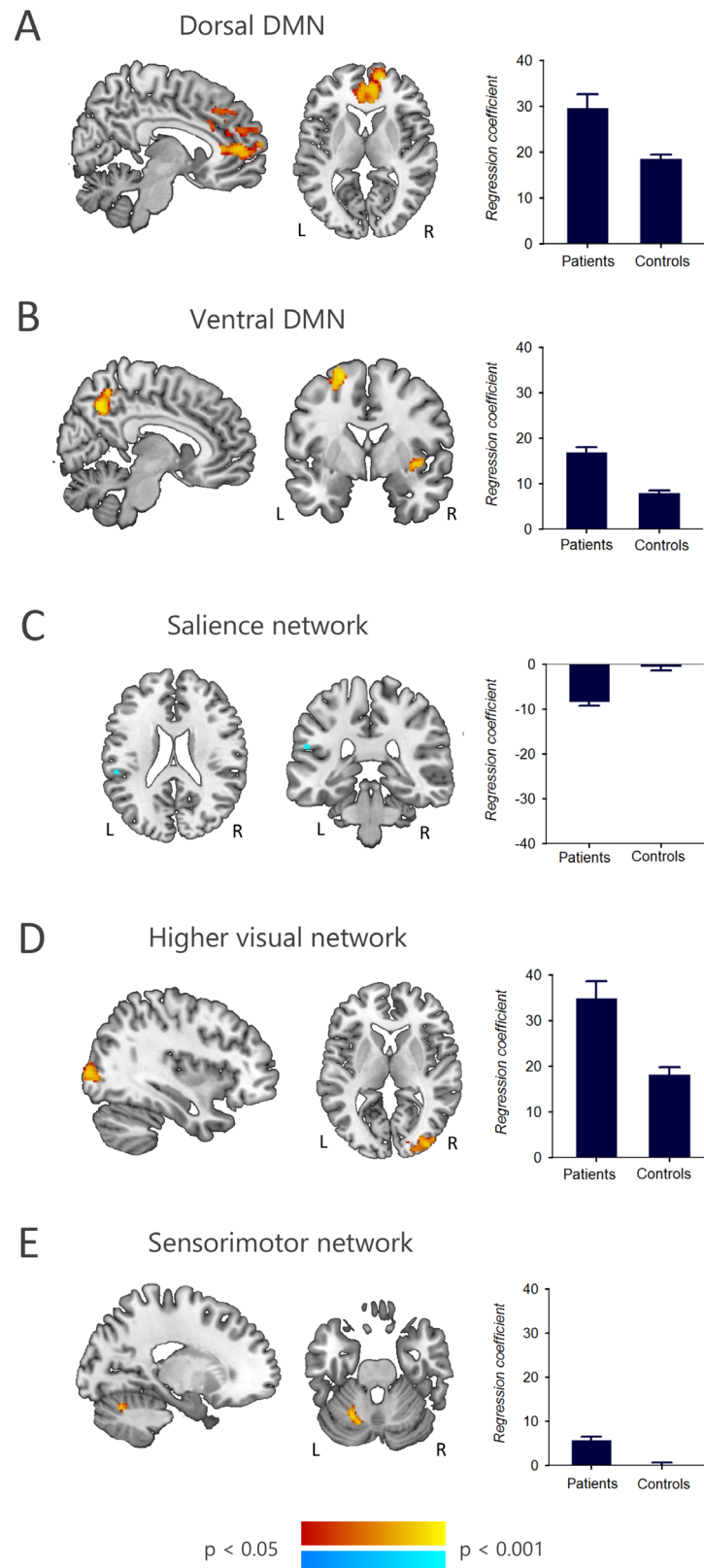
**Figure 2** Patients with anti-LGI1 encephalitis show aberrant functional connectivity in several large-scale networks. Five resting-state networks showed significant group differences between patients and controls: (A) In patients with anti-LGI1 encephalitis, functional connectivity was increased between the *dorsal DMN* and the aCC/pCC, the left precuneus and the mPFC and left precentral gyrus in the frontal cortex. (B) In the *ventral DMN*, patients had higher connectivity with distributed frontal areas (insula, left superior and right inferior frontal gyrus), the inferior temporal and right lateral occipital cortex. (C) Decreased connectivity was observed between the *salience network* and two clusters in the left parietal opercular and postcentral cortex. Moreover, (D) patients exhibited higher connectivity in the right lateral occipital cortex within the *visual network* and (E) the left cerebellum within the *sensorimotor network* (p<0.05; corrected for multiple comparisons). aCC/pCC, anterior/posterior cingulate cortex; DMN, default mode network; LGI1, leucine-rich glioma-inactivated 1; mPFC, medial prefrontal cortex.
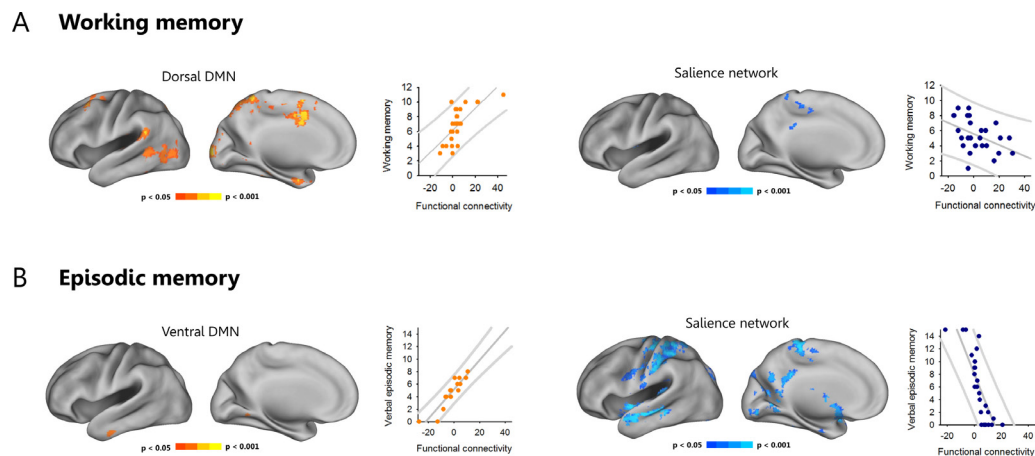
A **Working memory**



B **Episodic memory**



**Figure 3**  Correlations with memory performance. Alterations in functional connectivity significantly correlated with memory performance in patients with anti-LGI1 encephalitis (p<0.05; corrected for multiple comparisons). (A) Better working memory performance was associated with higher connectivity between the dorsal DMN and the left middle/superior temporal and parahippocampal gyrus, the left temporal pole as well as the cingulate cortex (digit span test, p=0.012). Likewise, episodic memory function was better with increased connectivity between the ventral fraction of the DMN and the left inferior temporal gyrus and fusiform cortex (RAVLT interference, p=0.005). This points to a potential functional compensatory mechanism. (B) In contrast, cognitive impairment was associated with aberrant SN connectivity: Higher insular connectivity and coactivation of temporal (hippocampus, middle and superior temporal gyrus) and parietal default mode areas (posterior cingulate cortex, precuneus, superior parietal lobule and right angular gyrus) predicted both impaired working memory (p=0.032) and impaired episodic memory (RAVLT sum score, p=0.007; delayed recall, p=0.002). DMN, default mode network; LGI1, leucine-rich glioma-inactivated 1; RAVLT, Rey Auditory Verbal Learning Test; SN, salience network.

were observed in the *left* and *right frontoparietal networks*, the *auditory network* and the *primary visual network*.

### Relationship between hippocampal structure and functional network changes

An interaction analysis revealed an aberrant structure-function relationship between left hippocampal volume and ventral DMN connectivity in patients compared with controls (p=0.029; figure 4). Specifically, patients showed increased connectivity in the retrosplenial cortex in association with smaller hippocampal volumes while the opposite effect was present for controls.

### DISCUSSION

We observed functional connectivity alterations in several major networks in patients with anti-LGI1 encephalitis, suggesting that the disease is not confined to the limbic system, but rather affects a wide range of brain regions and functional systems. Affected networks include not only the DMN, which is highly interconnected with the hippocampus, but also the SN, the sensorimotor network and the higher visual network. Increased connectivity of



**Figure 4**  Aberrant structural-functional relationship in anti-LGI1 encephalitis. (A) Interaction analysis revealed an inversed relationship between left hippocampal volume and retrosplenial cortex connectivity in the ventral default mode network. (B) In anti-LGI1 encephalitis, patients showed a negative slope of the regression, with smaller left hippocampus volume relating to higher retrosplenial connectivity.

the ventral and dorsal DMN was associated with better memory performance, suggesting a compensatory role of these network changes. The characteristic connectivity alterations in anti-LGI1 encephalitis may expedite the correct diagnosis after implementation in future routine imaging algorithms.

The most prominent connectivity changes were observed in the DMN. The DMN comprises a set of brain areas that activate in the absence of an experimental task and that are related to self-referential processing.[28] The network consists of a dorsal subsystem engaged in self-relevant mental simulations and a ventral subsystem implicated in episodic memory processing.[29 30] The hippocampus, the major disease target in anti-LGI1 encephalitis,[4 12] is part of the ventral DMN and also highly interconnected with dorsal DMN regions. In line with this, working memory and episodic memory deficits constitute the major domains of cognitive impairment in anti-LGI1 encephalitis.[4 9] Here, we correspondingly observed connectivity alterations in both DMN subsystems: Patients with anti-LGI1 encephalitis showed significantly increased functional connectivity between the precuneus and other *ventral DMN* regions as well as between the mPFC/ACC and other *dorsal DMN* areas. Interaction analyses revealed a disturbed structure-function relationship in patients, with an inverse association between left hippocampal volume and ventral DMN connectivity in the retrosplenial cortex. Our results suggest that focal structural hippocampal damage can induce functional connectivity alterations that propagate to distant brain regions. In addition, functional connectivity alterations can occur independent of hippocampal damage and might be the result of global LGI1 antibody-mediated effects. Indeed, although predominantly expressed in the CA3 and dentate gyrus subfields of the hippocampus, LGI1 is also found to a weaker extend throughout the inner layers of the cerebral cortex.[14]

Increased ventral and dorsal DMN connectivity was moreover associated with significantly better memory performance. In the dorsal DMN, increased connectivity with the cingulate cortex and further areas was related to better working memory performance while for the ventral DMN, left temporal lobe
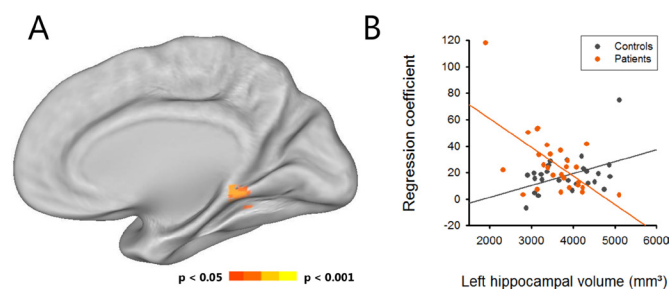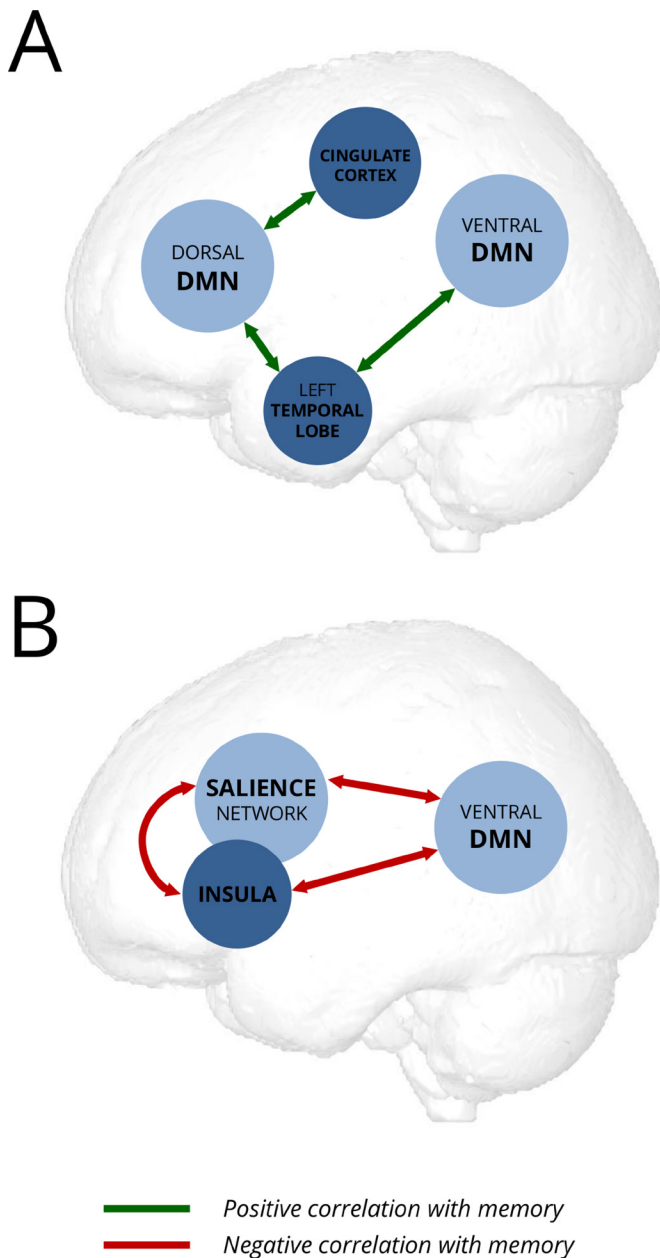
**Figure 5** Schematic model of potential compensatory (A) and maladaptive (B) changes of resting-state functional connectivity in anti-LGI1-encephalitis. DMN, default mode network.

in anti-N-methyl-D-aspartate receptor (NMDAR) encephalitis, another autoimmune encephalitis with (less severe) hippocampal atrophy, in which both hippocampi were decoupled from the DMN, with stronger decoupling relating to worse memory performance.[19 33] In addition to this hippocampal dysfunction, patients with anti-NMDAR encephalitis exhibit a characteristic pattern of whole-brain functional connectivity alterations—including reduced functional connectivity in the sensorimotor network, the visual network and the ventral attention network—likely reflecting the ubiquitous expression of NMDA receptors throughout the human brain.[33] This pattern is clearly distinguishable from the connectivity changes in anti-LGI1 encephalitis and indicates that functional connectivity analyses can identify unique and disease-specific connectivity profiles in autoimmune encephalitis.

Marked connectivity changes of the insula are another main finding of this study. Insular activity has been related to a wide spectrum of functions, including autonomic control, emotion processing and higher-level cognition.[34] Together with the dorsal anterior cingulate, the insula is a main hub of the SN, a functional network centrally involved in detecting relevant external stimuli and switching between the central executive network and the DMN to guide behaviour.[35] In the present analysis, the ventral DMN exhibited increased connectivity with the right insula. This increased connectivity was associated with impaired verbal episodic memory. Interestingly, the same principle applied to the SN: The higher the connectivity between insula and DMN regions, the worse patients performed on working memory and episodic memory tests. These results suggest that aberrant coupling of the insula and the SN with the DMN contributes to cognitive deficits in anti-LGI1 encephalitis (figure 5). In addition, around 26% of our patients experienced affective and/or behavioural symptoms including anxiety, mood changes and psychosis. Aberrant SN interactions have been reported across various neuropsychiatric diseases, including frontotemporal dementia and schizophrenia.[36] The observed connectivity changes of the insula might therefore also be linked to neuropsychiatric features in LGI1 encephalitis.[13 37 38] Furthermore, our observations extend previous reports of T2/FLAIR-hyperintense signal alterations in the insula in patients with anti-LGI1 encephalitis.[4 9 39 40] Interestingly, insular involvement was also linked to episodic bradycardia in three patients with anti-LGI1 encephalitis.[41] Together, these findings suggest a role for insula dysfunction in the pathophysiology of anti-LGI1 encephalitis that is linked to autonomic control as well as cognitive and behavioural function.

The cognitive deficits in anti-LGI1 encephalitis are not restricted to limbic dysfunction, that is, hippocampal damage-induced memory impairment. Indeed, attention, verbal fluency and executive functions can be equally affected.[4 42] Given the here reported aberrant interaction between the salience and the DMN, network models of cognitive function may provide a key to the understanding of the widespread cognitive dysfunction in autoimmune encephalitis. The insula as key node of the SN, for example, monitors and detects behaviourally relevant (salient) events. When a salient stimulus is detected, the right insula mediates the switch from the internally directed DMN to the externally directed frontoparietal executive network (FPN) to facilitate access to attentional and executive processing.[34] The FPN core regions, that is, lateral prefrontal cortex and posterior parietal cortex, support attentional processes and goal-directed behaviour during working memory updating, retrieval of episodic memories, shifting of attention and inhibiting motor responses.[43] For neurological diseases, accumulating evidence

connectivity was positively correlated with episodic memory performance. Such increased functional connectivity associated with better clinical symptoms or task performance has previously been established as potential functional compensatory mechanism in response to structural damage,[31] and has been observed in other neurological disorders with structural hippocampal damage. For example, patients with Alzheimer's disease showed increased connectivity in the ventral and dorsal DMN associated with better cognitive performance at early disease stages that was lost at follow-up with cognitive deterioration.[30] In patients with hippocampal sclerosis, increased connectivity within the DMN similarly related to better memory performance.[32] Thus, strengthened ventral and dorsal DMN connectivity may provide a compensatory mechanism for structural hippocampal damage in patients with anti-LGI1 encephalitis (figure 5). Interestingly, these findings contrast with the connectivity changes

suggests that disrupted saliency mapping contributes to cognitive dysfunction.[36] This line of research may elucidate the increased error susceptibility (as seen on the Go/No-Go task) in patients with anti-LGI1 encephalitis and, more generally, also help to explain cognitive impairments in patients with normal structural MRI.

Interestingly, our network analysis also identified increased connectivity between the sensorimotor network and the cerebellum in patients. A recent FDG-PET analysis reported hypermetabolism of the sensorimotor cortex in patients with anti-LGI1 encephalitis that, together with contralateral frontal EEG changes and results from polymyographic recordings, are suggestive of a motor cortex origin of FBDS.[5] Another FDG-PET study observed hypermetabolism in the precentral gyrus, basal ganglia and cerebellum in patients with LGI1 encephalitis with FBDS.[16] Here, precentral hypermetabolism was associated with higher disease severity at follow-up, suggesting that sensorimotor network integrity may serve as a predictor for disease-related disability. Although the sensorimotor network was altered in patients, the connectivity changes observed in our study did not significantly correlate with FBDS frequency, likely related to the fact that only three patients were still experiencing FBDS at the time of functional imaging. Transient FBDS-related changes in motor areas, such as the basal ganglia T1/T2 hyperintensities observed in 30%–40% of patients in previous studies, responded well to or dissolved completely following immunotherapy.[6 7] We therefore assume that FBDS-related motor cortex connectivity abnormalities are most pronounced during the FBDS stage itself. Taken together, functional connectivity alterations and metabolic changes of the sensorimotor system constitute another extralimbic manifestation of LGI1 encephalitis.

The target antigen of anti-LGI1 encephalitis was only recently discovered.[1] Due to delayed diagnosis, some of the patients did not receive immediate immunotherapy in the hospitals of their first presentation. Variable disease courses are thus a natural limitation of this study. In addition, we believe that future longitudinal studies will help to better understand the influence of therapeutic strategies on structural and functional brain changes in anti-LGI1 encephalitis and to establish causal inferences on compensatory or maladaptive functional connectivity.

In the present study, we observed that structural hippocampal damage is associated with a characteristic pattern of widespread functional network alterations in anti-LGI1 encephalitis. Connectivity changes correlated with memory performance and disease severity, corroborating the clinical relevance of our observations and suggesting successful compensatory mechanisms. Our results moreover suggest that resting state functional MRI and data-driven functional connectivity analyses might become useful clinical tools that can track disease-related changes in the brain and inform treatment monitoring. Finally, our findings offer an explanation why cognitive impairments are not restricted to memory dysfunction but can extend to attention and executive deficits, and they shed light on cases with cognitive deficits despite an unremarkable MRI.

**Author affiliations**
[1]Department of Neurology, Charité – Universitätsmedizin Berlin, Corporate member of Freie Universität Berlin, Humboldt-Universität zu Berlin, and Berlin Institute of Health, Berlin, Germany
[2]German Center for Neurodegenerative Diseases (DZNE), Berlin, Germany
[3]Department of Neurology, Hannover Medical School, Hannover, Germany
[4]Department of Neurology, University of Leipzig, Leipzig, Germany
[5]Department of Neurology, University Hospital Schleswig-Holstein, Lübeck, Germany
[6]Institute of Clinical Chemistry, University Hospital Schleswig-Holstein, Lübeck, Germany
[7]Neurocure Clinical Research Center and Experimental and Clinical Research Center, Max Delbrueck Center for Molecular Medicine and Charité – Universitätsmedizin Berlin, Berlin, Germany
[8]Berlin Center for Advanced Neuroimaging, Charité – Universitätsmedizin Berlin, Berlin, Germany
[9]Department of Neurology, Memory Disorders and Plasticity Group, University Hospital Schleswig-Holstein, Berlin, Germany
[10]Berlin School of Mind and Brain, Humboldt-Universität zu Berlin, Berlin, Germany

## REFERENCES

1 Lai M, Huijbers MG, Lancaster E, et al. Investigation of LGI1 as the antigen in limbic encephalitis previously attributed to potassium channels: a case series. *Lancet Neurol* 2010;9:776–85.
2 Irani SR, Alexander S, Waters P, et al. Antibodies to Kv1 potassium channel-complex proteins leucine-rich, glioma inactivated 1 protein and contactin-associated protein-2 in limbic encephalitis, Morvan's syndrome and acquired neuromyotonia. *Brain* 2010;133:2734–48.
3 van Sonderen A, Petit-Pedrol M, Dalmau J, et al. The value of LGI1, Caspr2 and voltage-gated potassium channel antibodies in encephalitis. *Nat Rev Neurol* 2017;13:290–301.
4 Finke C, Prüss H, Heine J, et al. Evaluation of cognitive deficits and structural hippocampal damage in encephalitis with leucine-rich, glioma-inactivated 1 antibodies. *JAMA Neurol* 2017;74:50–9.
5 Navarro V, Kas A, Apartis E, et al. Motor cortex and hippocampus are the two main cortical targets in LGI1-antibody encephalitis. *Brain* 2016;139(Pt 4):1079–93.
6 Flanagan EP, Kotsenas AL, Britton JW, et al. Basal ganglia T1 hyperintensity in LGI1-autoantibody faciobrachial dystonic seizures. *Neurol Neuroimmunol Neuroinflamm* 2015;2:e161.
7 Gadoth A, Pittock SJ, Dubey D, et al. Expanded phenotypes and outcomes among 256 LGI1/CASPR2-IgG-positive patients. *Ann Neurol* 2017;82:79–92.
8 Irani SR, Stagg CJ, Schott JM, et al. Faciobrachial dystonic seizures: the influence of immunotherapy on seizure control and prevention of cognitive impairment in a broadening phenotype. *Brain* 2013;136:3151–62.
9 van Sonderen A, Thijs RD, Coenders EC, et al. Anti-LGI1 encephalitis: clinical syndrome and long-term follow-up. *Neurology* 2016;87:1449–56.
10 Thompson J, Bi M, Murchison AG, et al. The importance of early immunotherapy in patients with faciobrachial dystonic seizures. *Brain* 2018;141:348–56.
11 Irani SR, Michell AW, Lang B, et al. Faciobrachial dystonic seizures precede Lgi1 antibody limbic encephalitis. *Ann Neurol* 2011;69:892–900.
12 Miller TD, Chong TT, Aimola Davies AM, et al. Focal CA3 hippocampal subfield atrophy following LGI1 VGKC-complex antibody limbic encephalitis. *Brain* 2017;140:1212–9.
13 Ariño H, Armangué T, Petit-Pedrol M, et al. Anti-LGI1-associated cognitive impairment: Presentation and long-term outcome. *Neurology* 2016;87:1–8.
14 Herranz-Pérez V, Olucha-Bordonau FE, Morante-Redolat JM, et al. Regional distribution of the leucine-rich glioma inactivated (LGI) gene family transcripts in the adult mouse brain. *Brain Res* 2010;1307:177–94.
15 Heine J, Prüss H, Bartsch T, et al. Imaging of autoimmune encephalitis--relevance for clinical practice and hippocampal function. *Neuroscience* 2015;309:68–83.
16 Wegner F, Wilke F, Raab P, et al. Anti-leucine rich glioma inactivated 1 protein and anti-N-methyl-D-aspartate receptor encephalitis show distinct patterns of brain glucose metabolism in 18F-fluoro-2-deoxy-d-glucose positron emission tomography. *BMC Neurol* 2014;14:136.
17 Biswal B, Yetkin FZ, Haughton VM, et al. Functional connectivity in the motor cortex of resting human brain using echo-planar MRI. *Magn Reson Med* 1995;34:537–41.
18 Raichle ME. Two views of brain function. *Trends Cogn Sci* 2010;14:180–90.

19 Finke C, Kopp UA, Scheel M, *et al*. Functional and structural brain changes in anti-N-methyl-D-aspartate receptor encephalitis. *Ann Neurol* 2013;74:284–96.

20 Graus F, Titulaer MJ, Balu R, *et al*. A clinical approach to diagnosis of autoimmune encephalitis. *Lancet Neurol* 2016;15:391–404.

21 Beckmann CF, Smith SM. Probabilistic independent component analysis for functional magnetic resonance imaging. *IEEE Trans Med Imaging* 2004;23:137–52.

22 Filippini N, MacIntosh BJ, Hough MG, *et al*. Distinct patterns of brain activity in young carriers of the APOE-epsilon4 allele. *Proc Natl Acad Sci U S A* 2009;106:7209–14.

23 Zhang Y, Brady M, Smith S. Segmentation of brain MR images through a hidden Markov random field model and the expectation-maximization algorithm. *IEEE Trans Med Imaging* 2001;20:45–57.

24 Winkler AM, Ridgway GR, Webster MA, *et al*. Permutation inference for the general linear model. *Neuroimage* 2014;92:381–97.

25 Smith SM, Nichols TE. Threshold-free cluster enhancement: addressing problems of smoothing, threshold dependence and localisation in cluster inference. *Neuroimage* 2009;44:83–98.

26 Shirer WR, Ryali S, Rykhlevskaia E, *et al*. Decoding subject-driven cognitive states with whole-brain connectivity patterns. *Cereb Cortex* 2012;22:158–65.

27 Beckmann CF, DeLuca M, Devlin JT, *et al*. Investigations into resting-state connectivity using independent component analysis. *Philos Trans R Soc Lond B Biol Sci* 2005;360:1001–13.

28 Raichle ME, MacLeod AM, Snyder AZ, *et al*. A default mode of brain function. *Proc Natl Acad Sci U S A* 2001;98:676–82.

29 Buckner RL, Andrews-Hanna JR, Schacter DL. The brain's default network: anatomy, function, and relevance to disease. *Ann N Y Acad Sci* 2008;1124:1–38.

30 Damoiseaux JS, Prater KE, Miller BL, *et al*. Functional connectivity tracks clinical deterioration in Alzheimer's disease. *Neurobiol Aging* 2012;33:828.e19–828.e30.

31 Schoonheim MM, Geurts JJ, Barkhof F. The limits of functional reorganization in multiple sclerosis. *Neurology* 2010;74:1246–7.

32 Bettus G, Guedj E, Joyeux F, *et al*. Decreased basal fMRI functional connectivity in epileptogenic networks and contralateral compensatory mechanisms. *Hum Brain Mapp* 2009;30:1580–91.

33 Peer M, Prüss H, Ben-Dayan I, *et al*. Functional connectivity of large-scale brain networks in patients with anti-NMDA receptor encephalitis: an observational study. *Lancet Psychiatry* 2017;4:768–74.

34 Menon V, Uddin LQ. Saliency, switching, attention and control: a network model of insula function. *Brain Struct Funct* 2010;214:655–67.

35 Seeley WW, Menon V, Schatzberg AF, *et al*. Dissociable intrinsic connectivity networks for salience processing and executive control. *J Neurosci* 2007;27:2349–56.

36 Menon V. Large-scale brain networks and psychopathology: a unifying triple network model. *Trends Cogn Sci* 2011;15:483–506.

37 Prüss H, Lennox BR. Emerging psychiatric syndromes associated with antivoltage-gated potassium channel complex antibodies. *J Neurol Neurosurg Psychiatry* 2016;87:1242–7.

38 Pollak TA, Moran N. Emergence of new-onset psychotic disorder following recovery from LGI1 antibody-associated limbic encephalitis. *BMJ Case Rep* 2017;2017:bcr2016218328.

39 Kotsenas AL, Watson RE, Pittock SJ, *et al*. MRI findings in autoimmune voltage-gated potassium channel complex encephalitis with seizures: one potential etiology for mesial temporal sclerosis. *AJNR Am J Neuroradiol* 2014;35:84–9.

40 Brown JW, Martin PJ, Thorpe JW, *et al*. Long-term remission with rituximab in refractory leucine-rich glioma inactivated 1 antibody encephalitis. *J Neuroimmunol* 2014;271:66–8.

41 Naasan G, Irani SR, Bettcher BM, *et al*. Episodic bradycardia as neurocardiac prodrome to voltage-gated potassium channel complex/leucine-rich, glioma inactivated 1 antibody encephalitis. *JAMA Neurol* 2014;71:1300.

42 Butler CR, Miller TD, Kaur MS, *et al*. Persistent anterograde amnesia following limbic encephalitis associated with antibodies to the voltage-gated potassium channel complex. *J Neurol Neurosurg Psychiatry* 2014;85:387–91.

43 Dodds CM, Morein-Zamir S, Robbins TW. Dissociating inhibition, attention, and response control in the frontoparietal network using functional magnetic resonance imaging. *Cereb Cortex* 2011;21:1155–65.